

1 Swelling-induced structural changes and  
2 microparticle uptake of gelatin gels probed by  
3 NMR and CLSM

4  
5 Carmine D'Agostino<sup>(a)\*†</sup>, Roberta Liuzzi<sup>(b)†</sup>, Lynn F. Gladden<sup>(a)</sup>, Stefano Guido<sup>(b)(c)\*</sup>  
6

7 <sup>(a)</sup>Department of Chemical Engineering and Biotechnology, University of Cambridge,  
8 Pembroke Street, Cambridge, CB2 3RA, UK

9 <sup>(b)</sup>Dipartimento di Ingegneria Chimica, dei Materiali e della Produzione Industriale,  
10 Università di Napoli Federico II, UdR INSTM, P.le Tecchio, 80, 80125, Napoli, Italy

11 <sup>(c)</sup>CEINGE Advanced Biotechnologies, via G. Salvatore 486, 80145 Napoli, Italy  
12

13 \*Corresponding Authors:

14 Dr Carmine D'Agostino

15 Department of Chemical Engineering and Biotechnology, University of Cambridge,  
16 Pembroke Street, Cambridge, CB2 3RA, UK, Email: [cd419@cam.ac.uk](mailto:cd419@cam.ac.uk), Tel: +44 (0)1223-  
17 334796  
18

19 Prof Stefano Guido

20 Dipartimento di Ingegneria Chimica, dei materiali e della produzione industriale, Università  
21 di Napoli Federico II, P.le Tecchio, 80, 80125, Napoli, Italy, Email: [steguido@unina.it](mailto:steguido@unina.it), Tel:  
22 +39 081-7682271  
23

24 † These two authors contributed equally to this work and are co-first authors.  
25  
26  
27  
28

29  
30  
31  
32  
33  
34  
35  
36  
37  
38  
39  
40  
41  
42  
43  
44  
45  
46  
47  
48  
49  
50  
51  
52  
53  
54  
55  
56  
57

**Abstract**

Gelatin gels are increasingly involved in many industrial applications due to several advantages including cost efficiency and biocompatibility. Generally, their production requires the use of aqueous solvents, which cause a significant swelling, due to the ability of solvent molecules to penetrate through the gel microstructure and increase its volume. Since swelling mechanisms and their effect on gel structure are not fully understood, further investigations are required. In this work, we combine macroscopic measurements of the swelling ratio (SR) with Nuclear Magnetic Resonance (NMR) and Confocal Laser Scanning Microscopy (CLSM) to investigate changes in gelatin structure as a function of both polymer concentration and swelling time. SR values increase as a function of time until a maximum is reached and then show a slight drop for all the gelatin concentrations after 24 h swelling time, probably due to a network relaxation process. NMR allows to determine mass transport and molecular dynamics of water inside the gelatin pores, while CLSM is used to visualize the penetration of tracers (polystyrene microbeads) with diameter much larger than the gel pores. Structural parameters, such as average pore size and tortuosity, are estimated. In particular, the pore size decreases for higher polymer concentration and increases during swelling, until reaching a maximum, and then dropping at longer times. The penetration of tracers provides evidence of the heterogeneity of the gel structure and shows that single microcarriers can be loaded in gelatin gels upon swelling.

**Keywords:** Gelatin gel, Swelling, Water mobility, Mesh size, NMR, Confocal Microscopy

## 59 INTRODUCTION

60 Gelatin is an animal protein derived from a partial hydrolysis of collagen, one of the main  
61 components of bones, skin, connective tissues and extracellular matrix. Based on the source<sup>1</sup>  
62 and on the pre-treatment of collagen, acid or alkaline, two different types of gelatin can be  
63 obtained, Type A and B, respectively. Although the amino acid composition is similar to that  
64 of the native collagen, the organization of the macromolecules (overlapping and cross-linked  
65 triple helices) is very different due to the manufacturing processes.<sup>2, 3</sup> At temperature above  
66 40-50 °C gelatin is in a sol state while it forms an elastic gel by lowering the temperature  
67 below 30 °C, allowing a partial renaturing of collagen in a thermo-reversible manner.  
68 Moreover, factors such as humidity, initial gelatin concentration, temperature<sup>4</sup> and addition of  
69 cross-linkers can easily affect the final structure of the gelatin.<sup>5</sup>

70 Due to its versatility, gelatin is widely used in many applications including in the food  
71 industry,<sup>6, 7</sup> as ingredient or for confectionary, photographic, pharmaceutical and medical  
72 fields.<sup>8</sup> In the latter case, due to the biocompatibility and low costs, the use of gelatin is  
73 required not only as shell of hard or soft capsules, tablets and dietary supplements but also as  
74 scaffold for tissue engineering,<sup>9, 10</sup> for example as skin substitute<sup>11</sup> or cartilage  
75 regeneration.<sup>12, 13</sup> Despite the applications of gelatin are constantly increasing, there are still  
76 gaps in the full understanding of its structure and structure-related mechanisms.

77 Swelling of gelatin is one of the main processes responsible for its large use in industry. It has  
78 been demonstrated that this process depends on many factors, including temperature,<sup>14</sup> salt  
79 concentration in the solvent,<sup>15</sup> pH and charge distribution.<sup>16</sup> If cross-linkers are added,<sup>17, 18</sup>  
80 swelling is also affected by the cross-linker to gelatin mass ratio,<sup>15, 19</sup> thus resulting in a  
81 reduced water uptake, up to 50-60%, and a higher stiffness.<sup>20</sup> Swelling is determined by the  
82 ability of solvent molecules to intercalate between chains and disrupt inter-chains bonds  
83 forming hydrogen bonds with the amide groups of gelatin. This disruption allows the gel to  
84 swell, adsorbing a large amount of water. It has been noticed that the swelling rate of  
85 hydrogels is faster near the free edges compared to the centre of the gel.<sup>21</sup> When the  
86 equilibrium is reached, the excessive water is free to move in the large pores and between  
87 helices, which is also known as “free water” or “bulk water”.<sup>22</sup> Swelling kinetics is generally  
88 described with a second-order equation<sup>16</sup> controlled by diffusion of the solvent (water) and  
89 relaxation of the macromolecule chains.<sup>23</sup> However, all these studies have been focused on

90 the swelling equilibrium behaviour of chemically or physically cross-linked gel due to their  
91 higher stability.<sup>24</sup>

92 In understanding and rationalizing the macroscopic behaviour of gelatin, transport as well as  
93 structural properties of these systems, including pore size and pore network connectivity, are  
94 among the main aspects to consider, especially when gelatin is used as a medium for drug  
95 delivery. These parameters have been investigated by several techniques including electron  
96 microscopy imaging,<sup>25, 26</sup> dynamic light scattering or diffusion of labelled molecules of  
97 different sizes and molecular weights.<sup>27</sup> The former requires image analysis for pore size  
98 estimation, while in the latter diffusion of the labelled molecules is used as a marker to  
99 estimate pore dimensions and connection, based on the ability of the fluorescent marker to  
100 penetrate, together with the solvent, inside the gel.

101 Studies on gel samples by NMR have been so far focused on the determination of the gel  
102 point,<sup>28</sup> on cross-linked gel<sup>29</sup> or on the role of the solvent during gelation.<sup>30</sup> Different states of  
103 water have been identified in the gel. Water can be strongly entrapped in the helix becoming  
104 a structural part of the gel, thus its mobility is very slow; it can locate between helices whose  
105 movement is faster; or it can be significantly far from the interface of the network such that is  
106 not affected by it, therefore retaining the molecular dynamics of free bulk water.<sup>31</sup>  
107 Discrepancies on the real existence of all these states in the gel are still a matter of debate,  
108 each case being dependent on the specific conditions. Therefore, a complete overview on  
109 alteration of the gelatin structure following different mechanisms is still lacking.

110 In this work, NMR is presented as non-invasive, powerful technique to study molecular  
111 dynamics of water inside gelatin structures. In particular, we use spin-lattice relaxation  
112 measurements,  $T_1$ , and pulsed-field gradient (PFG) NMR diffusion measurements to probe  
113 rotational and translation dynamics of water confined in gelatin structures, studying the effect  
114 of different parameters, most notably, polymer concentration and swelling time. In addition,  
115 possible changes in the gelatin structure due to diffusion of polystyrene particles of different  
116 dimensions are also investigated by both NMR and CLSM. Self-diffusion coefficient of  
117 water, average pore size and tortuosity of the porous matrix for all the samples are also  
118 estimated.

119

120

121

## 122 **MATERIALS AND METHODS**

### 123 **Materials**

124 Type A gelatin was available commercially by Extraco Gelatin under the trade name of  
125 Geltec (UG-719- H) derived from collagenous tissue by acid treatment and supplied in  
126 powder form. The molar mass of the gelatin is  $1.4 \times 10^5 \text{ g mol}^{-1}$ .

127 Mineral oil was purchased from Sigma-Aldrich. Polystyrene particles with diameter of 0.1  
128  $\mu\text{m}$  and 1  $\mu\text{m}$  were supplied, respectively, by Sigma-Aldrich and Bangs Laboratories Inc.  
129 Particle solutions were obtained by suspending particles in aqueous buffer at a solid  
130 concentration of 1%. For CLSM experiments, fluorescent polystyrene particles of 0.1  $\mu\text{m}$   
131 (Polyscience) and 1  $\mu\text{m}$  (Sigma-Aldrich) were prepared in suspension as in the previous case.

132

### 133 **Methods**

#### 134 **Gelatin solution preparation**

135 Gelatin solutions at concentrations of 10, 15, 20 and 30% by weight were obtained by  
136 dissolving a proper amount of gelatin powder in distilled water under gentle stirring for 1 h at  
137 60 °C until a homogeneous solution was obtained.

138

#### 139 **Swelling measurements**

140 Gelatin solutions obtained as previously described were injected in a glass mold  
141 (25×15×1mm) and cooled slowly at room temperature until complete gelation. Since the  
142 gelation time depends on the polymer concentration, a conservative gelation time of  
143 approximately 1 h was used for all the samples. Specimens were collected from the mold,  
144 transferred, soaked, and maintained at room temperature (about 25 °C) in different aqueous  
145 buffer solutions until equilibrium was achieved. A thin layer of mineral oil was applied at the  
146 bottom of the reservoir in order to avoid gel sticking. Permeability of mineral oil in water is  
147 very low and its use is advised when water loss from hydrogel has to be minimized.<sup>21</sup>  
148 Swelling was measured gravimetrically. At different time intervals, samples were collected  
149 from the aqueous buffer solutions and weighed. Excess solvent was removed gently with a  
150 filter paper. The total length of the experiments was 72 h. The swelling ratio was estimated  
151 according to the following equation:

$$152 \quad SR\% = \left( \frac{W_t - W_0}{W_0} \right) \times 100 \quad (1)$$

153 where  $W_t$  is the weight of the swollen gel at time  $t$  and  $W_0$  is the initial weight of the sample.

154

155 **Effect of polymer concentration and swelling time probed by NMR**

156 For NMR measurements of gelatin at different polymer concentrations, in the range 10-30%  
157 by weight, gelatin solutions were directly injected in the NMR tube (4 mm) and allowed to  
158 gel, avoiding formation of air bubbles. Gels were directly prepared in the NMR tubes also to  
159 avoid possible breaking or alteration of the structure during the insertion in the tube. For the  
160 investigation of the swelling effect, gelatin at 30% by weight was allowed to gel and then  
161 small cylinder punches with 2 mm diameter and 3 cm length, were allowed to swell in  
162 aqueous solution and were then collected after 2, 5, 18, 24, 48 and 72 h before being gently  
163 inserted into the NMR tubes.

164 **Effect of solid particle penetration probed by NMR**

165 Gelatin at 30% by weight was prepared directly into the NMR tubes as previously described.  
166 After gelation, 200  $\mu$ L of polystyrene particle solution at 1% was added on the top of the gel  
167 and samples were then sealed and kept at room temperature for 24 h. After this time, part of  
168 the solution was adsorbed by the sample due to the swelling, while excessive solution was  
169 removed and the sample analyzed by NMR.

170

171

172 **Effect of solid particle penetration probed by CLSM**

173 For CLSM experiments, gelatin at 30% by weight was prepared directly in a Ibidi  $\mu$ -slide  
174 multi-well (9.4 $\times$ 10.7 $\times$ 6.8 mm) and allowed to gel. After gelation, half of the sample was  
175 removed with the aid of a knife and the empty zone replaced with fluorescent particle  
176 solutions. Samples were kept sealed in order to prevent water evaporation from the solution  
177 and drying of the gel. For the first two hours a time lapse was acquired in brightfield by an  
178 inverted Leica TCS SP5 CLSM equipped with an Ar laser and a 20 $\times$  objective starting from  
179 the interface between the gel and the solution in order to follow the swelling of the interface.  
180 The delay time between acquisitions was of 1 min. After 24 h samples were analyzed in order  
181 to investigate the ability of particles of different dimensions to penetrate the gel network and  
182 assess possible changes in the gel structure. Images were acquired with a 63 $\times$  oil immersion  
183 objective along the entire gel sample and the maximum distance reached by particles was  
184 estimated. The density of particles was measured by dividing the number of particles by the  
185 image area in  $\mu\text{m}^2$ . This operation was repeated for 11 images at different depths in the

186 sample and the mean density was estimated. Image analysis was carried out using the  
187 commercial software Image Pro Plus 6.0. Results about the ability of particles to penetrate the  
188 gel were then compared with NMR results on water diffusion and relaxation properties within  
189 the gel in the presence of particles.

190

## 191 **NMR experiments**

192 All the NMR experiments were performed at room temperature on a Bruker Biospin DMX  
193 300 operating at a  $^1\text{H}$  frequency of 300.13 MHz using a Bruker Biospin Diff-30 diffusion  
194 probe capable of producing magnetic field gradient pulses up to  $11.76 \text{ T m}^{-1}$ . NMR  $T_1$   
195 relaxation times were measured using the standard inversion recovery pulse sequence.<sup>32</sup> The  
196  $T_1$  relaxation time constant was obtained by fitting the experimental data on the NMR signal  
197 intensity as a function of the time delay,  $S(t)$ , to the equation:<sup>32</sup>

$$198 \quad S(t) = S_0 \left[ 1 - 2 \exp\left(-\frac{t}{T_1}\right) \right] \quad (2)$$

199  $^1\text{H}$  PFG NMR diffusion measurements were performed using the alternating pulsed gradient  
200 stimulated echo (APGSTE) sequence<sup>33</sup> in order to minimize the effects of background  
201 magnetic field gradients. The measurements were carried out holding the gradient pulse  
202 duration,  $\delta$ , constant and varying the magnetic field gradient strength,  $g$ . The gradient pulse  
203 duration,  $\delta$ , was set to 1 ms. For each sample, the observation time,  $\Delta$ , was varied from 20 to  
204 1600 ms and no significant differences in the PFG log attenuation plots were observed, which  
205 implies that the self-diffusion coefficient of water inside the porous gelatin is essentially  
206 independent of the observation time (see Supplementary Information S1). Values of the  
207 diffusion coefficient,  $D$ , were obtained by fitting the PFG NMR experimental data to the  
208 expression:<sup>34</sup>

$$209 \quad \frac{E(g)}{E_0} = \exp\left[-D\gamma^2 g^2 \delta^2 (\Delta - \delta/3)\right] \quad (3)$$

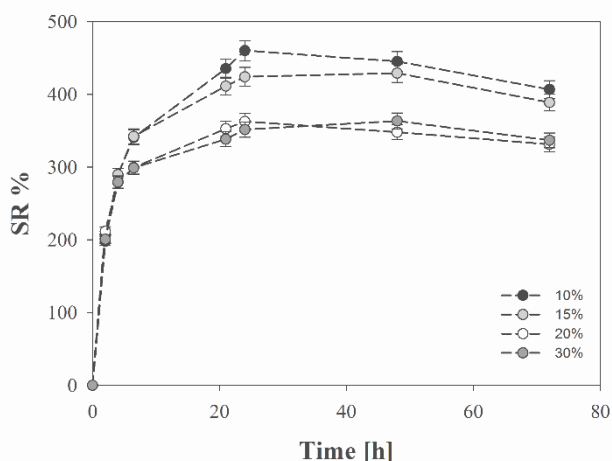
210 where  $E(g)$  and  $E_0$  are the NMR echo signal intensity in the presence and absence of  
211 magnetic field gradient, respectively.

212

## 213 **RESULTS AND DISCUSSION**

## 214 Swelling ratio

215 The swelling ratio (SR), quantified using Equation (1), as a function of time for gel samples  
216 at concentrations ranging from 10 to 30%, is reported in Figure 1. The results indicate an  
217 increase of adsorbed water for gels with lower polymer concentration. Initially, all trends  
218 overlap, showing a fast swelling rate. After 2 h, the trends show a lower swelling rate and  
219 start to differentiate from each other, until reaching an equilibrium state. Samples at 20% and  
220 30% polymer concentration show a similar trend, with a slight difference around 48 h, where  
221 the 20% gel shows a slightly lower SR. It is worth mentioning that for all samples, at longer  
222 time the equilibrium value tends to drop slightly. Although such a drop is not large, it is  
223 observed in all cases. This result could suggest that the excessive water in the sample leads to  
224 a slight weakness of the network. This effect is more pronounced for the 10% gel, which  
225 starts to drop after already 24 h, while the other samples generally show a similar behaviour  
226 after a longer swelling time. This can be explained by the higher amount of the polymer,  
227 which guarantees a higher stability and starts to relax at longer times.<sup>35</sup>



228

229 **Figure 1.** Swelling ratio of gelatin samples at 10%, 15%, 20% and 30% by weight polymer  
230 concentration.

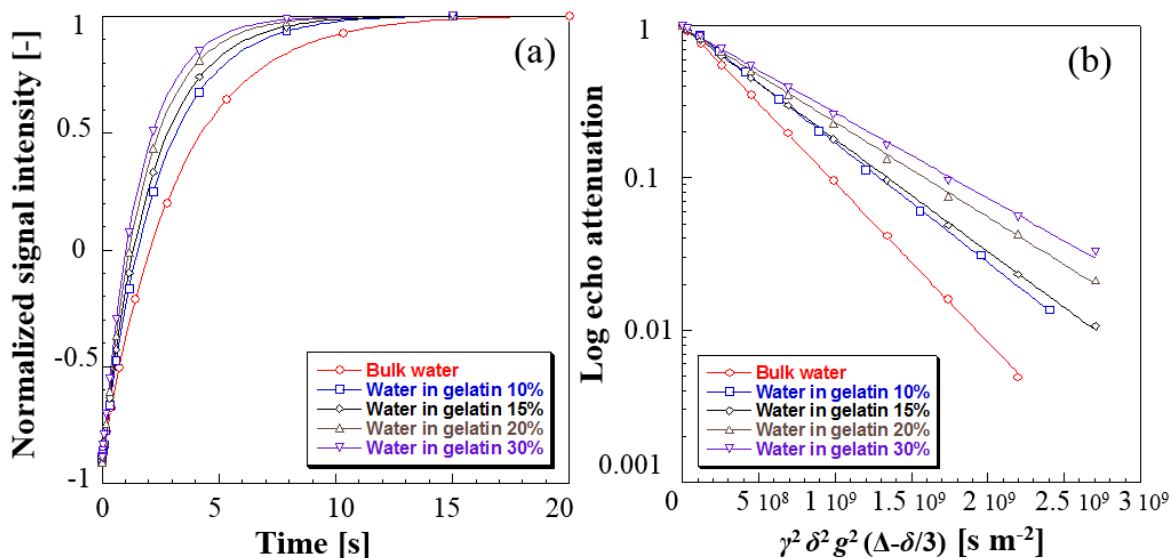
231

## 232 Effect of gelatin concentration

233 Figure 2 shows typical  $T_1$  inversion recovery (Figure 2a) and PFG diffusion log attenuation  
234 plots (Figure 2b) of water within the gelatin structure at different polymer concentrations.  
235 Plots for the other samples are of similar quality. The plots in Figure 2 clearly show  
236 significant changes of relaxation and diffusion properties of water as the polymer  
237 concentration increases. By inspection of the plots, it is already possible to see as, relatively

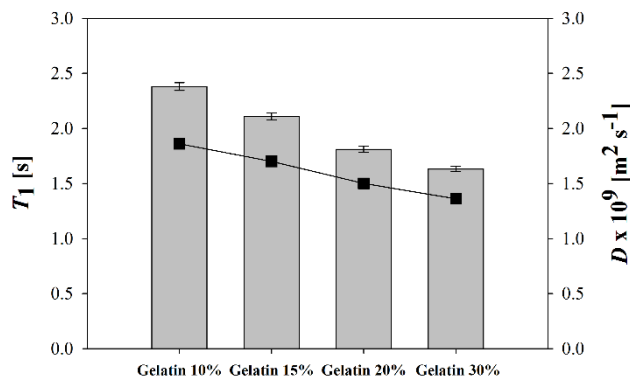


238 to water confined within the gelatin structures, bulk water has a significantly longer  $T_1$ , i.e.,  
 239 slower recovery of magnetization in Figure 2a, and a higher self-diffusion coefficient, i.e., a  
 240 steeper slope in Figure 2b. As the polymer concentration increases, the  $T_1$  of water becomes  
 241 shorter and its self-diffusion coefficient slower, which indicates a slowing down of molecular  
 242 dynamics due to the confinement within the gelatin pore structure.



243  
 244 **Figure 2.** (a)  $T_1$  inversion recovery and (b) PFG log attenuation plots of water in gelatin at  
 245 different polymer concentration. Solid lines are fitting to: (a) Equation (2) and (b) Equation  
 246 (3).

247  
 248 From the data in Figure 2, using Equations (2) and (3), it is possible to evaluate the values of  
 249 the  $T_1$  relaxation time and self-diffusion coefficient,  $D$ , of water as a function of polymer  
 250 concentration, which are reported in Figure 3.



252 **Figure 3.**  $T_1$  relaxation time (columns) and self-diffusion coefficient  $D$  (squares) of water  
 253 inside gelatin with different polymer concentration. For free bulk water  $T_1 = 3.22$  s and  $D =$   
 254  $2.35 \times 10^{-9} \text{ m}^2 \text{ s}^{-1}$ . The solid line is a guide to the eye.

255  
 256 It is clear that as the percentage of polymer increases, both the  $T_1$  and  $D$  values decrease,  
 257 which is consistent with a reduced rotational and translational dynamics<sup>36</sup> of water molecules  
 258 as the polymer concentration increases. In particular, the observed  $T_1$  relaxation rate can be  
 259 written as:<sup>37</sup>

$$260 \quad \frac{1}{T_1} = \frac{1}{T_{1,\text{bulk}}} + \frac{S}{V} \rho_1 \quad (4)$$

261 where  $1/T_{1,\text{bulk}}$  is the relaxation rate of the bulk fluid and, once the temperature is fixed, this is  
 262 a constant,  $\rho_1$  is the surface relaxivity, which is a property of the material and for the system  
 263 under investigation can be assumed to be constant across the samples, and  $S/V$  is the surface-  
 264 to-volume ratio of the gelatin structure. Therefore, a decrease in  $T_1$ , that is, an increase of the  
 265  $1/T_1$  relaxation rate, implies an increase of  $S/V$ .

266 In order to further investigate the diffusive behaviour of water inside the gelatin structure,  
 267 PFG NMR experiments were carried for a range of different observation times,  $\Delta$ , and the  
 268 results are reported in Table 1.

269 **Table 1.** Self-diffusion coefficient,  $D$ , of water for gelatin with different polymer  
 270 concentration as a function of the observation time,  $\Delta$ .

	Self-diffusion coefficient, $D$ , [ $\text{m}^2 \text{ s}^{-1}$ ] $\times 10^9$			
	$\Delta = 20$ ms	$\Delta = 200$ ms	$\Delta = 800$ ms	$\Delta = 1600$ ms
<b>Gelatin 10%</b>	$1.89 \pm 0.05$	$1.86 \pm 0.05$	$1.83 \pm 0.05$	$1.87 \pm 0.05$
<b>Gelatin 15%</b>	$1.74 \pm 0.04$	$1.70 \pm 0.04$	$1.70 \pm 0.04$	$1.71 \pm 0.04$
<b>Gelatin 20%</b>	$1.54 \pm 0.04$	$1.50 \pm 0.04$	$1.47 \pm 0.04$	$1.48 \pm 0.04$
<b>Gelatin 30%</b>	$1.40 \pm 0.04$	$1.36 \pm 0.03$	$1.35 \pm 0.03$	$1.34 \pm 0.03$

271  
 272 The results in Table 1 clearly show that the self-diffusion coefficient of water in the gelatin  
 273 samples is lower than that of bulk water,  $2.35 \times 10^{-9} \text{ m}^2 \text{ s}^{-1}$ , and is essentially independent of  
 274 the observation time. This result, together with the lack of curvature of the PFG plots (Figure  
 275 2b) implies that already at 20 ms water molecules are probing regions of the pore space that  
 276 are representative of the whole porous structure. Indeed, the root mean square displacement,

277  $RMSD = \sqrt{2D\Delta}$ , calculated at 20 ms is already of the order of tens of  $\mu\text{m}$ , which is far  
278 greater than the typical pore size for these gelatin systems, which of the order of tens of nm.<sup>38</sup>  
279 Hence, within the probed observation time, molecules experience many collisions with the  
280 pore walls and their diffusion is reduced by the presence of the pore network.<sup>36</sup> This  
281 behaviour is typical of mesoporous systems with a macroscopically homogeneous pore  
282 structure and is referred to as *quasi-homogeneous* behaviour.<sup>36, 39</sup> For the following analysis,  
283 values of  $D$  at 200 ms were considered.

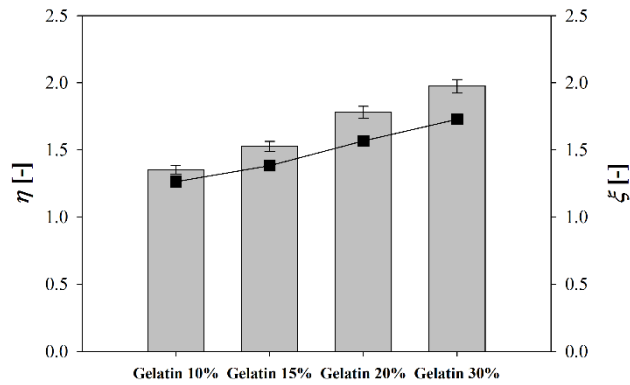
284 In order to obtain more insights into the effect of polymer concentration on the pore network  
285 properties, we define the following parameters:<sup>36</sup>

$$286 \quad \eta = \frac{T_{1,\text{bulk}}}{T_{1,\text{pore}}} \quad (5)$$

$$287 \quad \xi = \frac{D_{\text{bulk}}}{D_{\text{pore}}} \quad (6)$$

288 In the above expressions, the subscript “bulk” indicates free bulk water whereas the subscript  
289 “pore” indicates water confined within the gelatin pore network. The  $\eta$  parameter may be  
290 considered as an indication of the extent to which rotational dynamics of molecules within  
291 the pore network is reduced relative to the bulk.<sup>36</sup> The parameter  $\xi$  is the so-called PFG  
292 interaction parameter,<sup>36, 40</sup> which indicates the extent to which translational dynamics of  
293 molecules within the pore network is reduced relative to the bulk and can be considered a  
294 measure of the apparent tortuosity of the porous media, that is, the tortuosity experienced by  
295 water molecules diffusing within the pore network. Both parameters have been previously  
296 used to understand and explain changes in molecular dynamics of various fluids in different  
297 porous materials.<sup>36</sup> For fluids in pores behaving as bulk fluids both parameters are equal to  
298 one; an increase of such parameters inside pore structures indicates a slower molecular  
299 dynamics. The values of these parameters for water within the gelatin samples under  
300 investigation in this work are reported in Figure 4.

301



302

303 **Figure 4.** Values of  $\eta$  (columns) and  $\xi$  (squares) parameters of water in gelatin with different  
 304 polymer concentration. For water behaving as free bulk water  $\eta$  and  $\xi$  are equal to one. The  
 305 solid line is a guide to the eye.

306

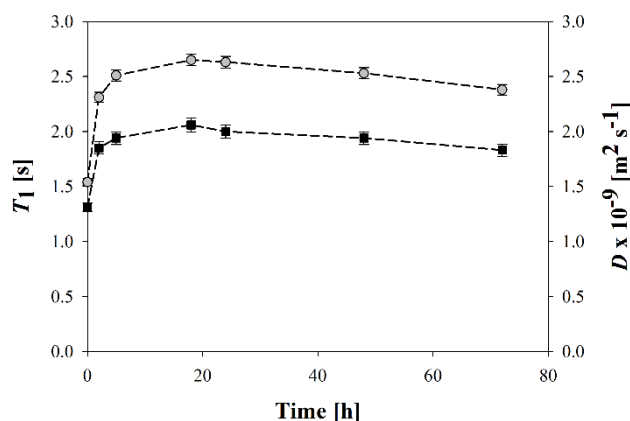
307 From Figure 4 two important conclusions can be drawn: (i) the increase in polymer  
 308 concentration reduces the rotational dynamics of water inside the gelatin relative to the bulk  
 309 fluid, indicating an increase in porosity and surface-to-volume ratio,  $S/V$ , of the pore  
 310 structure, which could be due either to an increase of contact surface area of water with the  
 311 gelatin, due to the increase of polymer amount, but also to a reduction of pore size as the  
 312 polymer concentration increases; (ii) at the same time, the increase in polymer concentration  
 313 is changing the pore network connectivity, with a more tortuous pore structure at higher  
 314 polymer concentrations, that is, higher values of  $\xi$ .

315

### 316 **Effect of swelling time**

317 It is now interesting to analyze the effect of swelling time over the molecular dynamics of  
 318 water inside the porous gelatin structure and on the properties of the pore structure itself.

319 These results are reported in Figure 5.

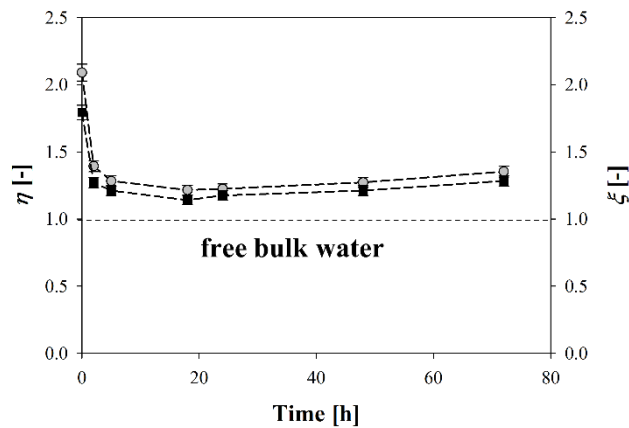


320

321 **Figure 5.**  $T_1$  relaxation time (circles) and self-diffusion coefficient  $D$  (squares) of water in  
 322 gelatin 30% sample as a function of the swelling time.

323

324 From Figure 5 it is possible to observe that both  $T_1$  and  $D$  increase rapidly in the first 5 h of  
 325 swelling. Such values reach an apparent plateau but then experience a slight decrease at  
 326 longer times, with values at 72 h swelling being lower than those recorded in the range 20-40  
 327 h. This behaviour is similar to that of the SR as a function of time, reported in Figure 1 and  
 328 strongly suggests a link between the NMR measured quantities and the macroscopic  
 329 measured SR. The changes in  $T_1$  and  $D$  imply that the swelling time is having two main  
 330 effects on the pore structure. Firstly, the increase in  $T_1$  clearly suggests that as the swelling  
 331 proceeds, the rotational dynamics of water inside the pore becomes closer to that of bulk  
 332 water, the latter having a value of  $T_1 = 3.22$  s. Given that in this case the polymer  
 333 concentration is the same, this effect can be explained by an increase in the average pore size,  
 334 with a consequent decrease of  $S/V$ , as suggested by Equation (4). This implies that the effect  
 335 of the gelatin surface (i.e., surface relaxivity) on water molecular dynamics decreases and the  
 336 fluid behaves more like the free bulk fluid. In addition, the increase in swelling time is also  
 337 increasing the diffusion coefficient of water inside the pore structure, which, analogously to  
 338 the  $T_1$  behaviour, becomes closer to the self-diffusion coefficient of free bulk water, the latter  
 339 having a value of  $2.35 \times 10^{-9} \text{ m}^2 \text{ s}^{-1}$ . These findings are in good agreement with what has been  
 340 previously suggested when studying swelling of hydrogel.<sup>22, 41</sup> The values of the  $\eta$  and  $\xi$   
 341 parameters for gelatin samples at different swelling times are reported in Figure 6.



342

343 **Figure 6.** Values of  $\eta$  (circles) and  $\xi$  (squares) parameters of water in gelatin 30% sample as  
 344 a function of swelling time. For water behaving as free bulk water  $\eta$  and  $\xi$  are equal to one  
 345 (black dotted line).

346

347 From Figure 6 it is possible to observe that as the swelling time increases the value of  $\eta$  starts  
 348 to decrease approaching one, which implies that the rotational dynamics of water inside the  
 349 porous gel becomes closer to that of free bulk water. As previously explained, this can be  
 350 attributed to an enlargement of the pore structure and consequent increase of the average pore  
 351 size. The trend for the apparent tortuosity,  $\xi$ , is very similar to that observed for  $\eta$ , which  
 352 implies that the swelling of the porous matrix improves pore network connectivity and hence  
 353 improving water mass transfer by diffusion. However, at longer time such values start  
 354 experiencing a slight increase. The increase in such values is subtle but significant and is  
 355 observed for both parameters and could be attributed to a shrinking of the pore network due  
 356 to a possible relaxation of the structure. This is indeed supported by the results on the SR  
 357 shown in Figure 1, which indeed suggest a slight relaxation at a macroscopic level of the pore  
 358 structure after the initial swelling. This finding is significant because it highlights a link  
 359 between changes in microscopic properties of the gelatin, probed using NMR methods, and  
 360 macroscopic changes in the SR with time. It is important to point out that in order to confirm  
 361 the results reported in Figures 5 and 6, NMR measurements of  $T_1$  and  $D$  were repeated  
 362 several times, using the same samples but also with different batches. The results and the  
 363 trend were consistent and confirmed in all cases.

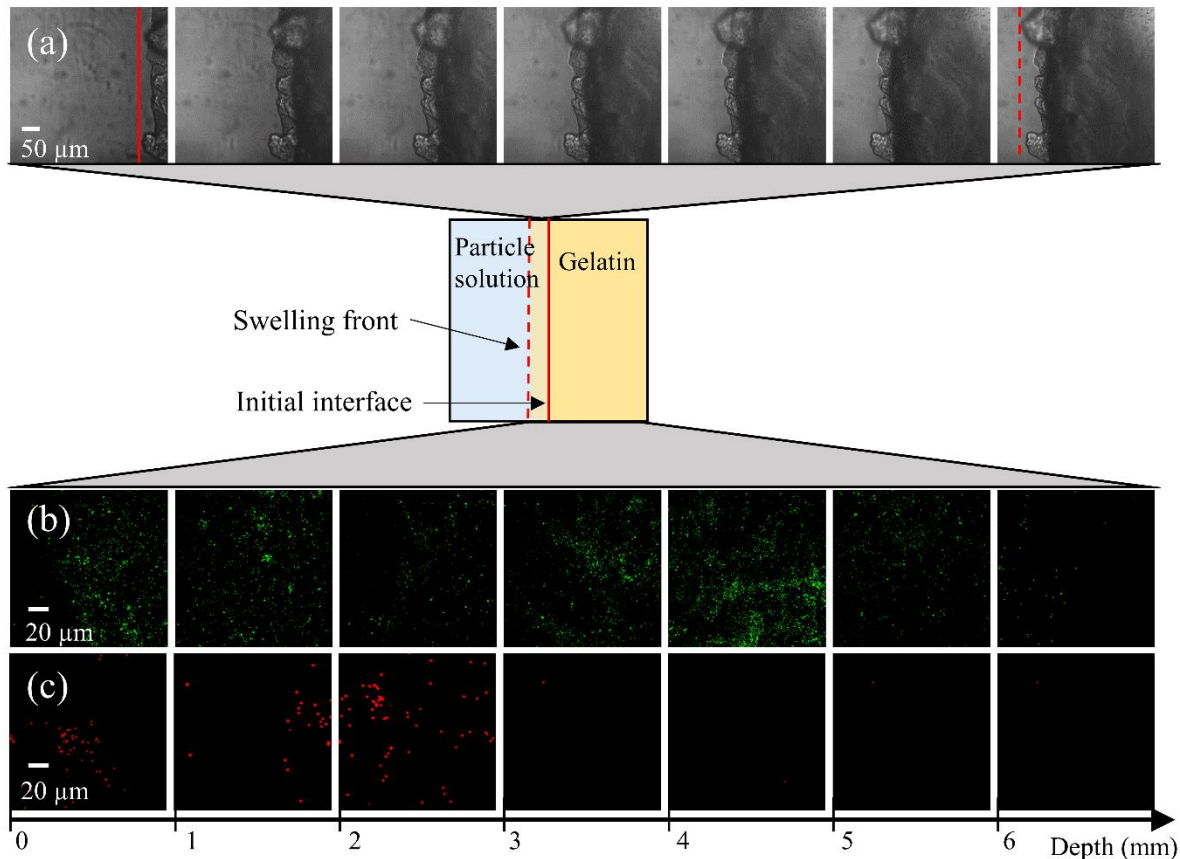
364

365

## 366 **Polystyrene particle permeation experiments**

367 Penetration of fluorescent polystyrene particles of two different dimensions, 0.1  $\mu\text{m}$  and 1  
368  $\mu\text{m}$  diameter, in a 30% gelatin gel were used as models to investigate possible changes in the  
369 gel structure. A similar approach can be useful to mimic the behaviour of polymeric particles  
370 when used as carriers for active principles during drug-loaded gels and delivery,<sup>42</sup> the latter  
371 dependent on the degree and rate of swelling as well as on gelatin concentration and gelatin-  
372 particles interaction. A schematic representation of our setup and results are reported in  
373 Figure 7. Firstly, the swelling of the gel interface was recorded during a 2 h time lapse with a  
374 delay time of 1 min (Figure 7a). It is possible to observe that the gel interface slides quickly  
375 according with the results in Figure 1, where the first 2 hours show a higher swelling rate. All  
376 other faces of the sample are immobilized by the walls and therefore cannot swell except for  
377 the upper face in contact with air, which is free to swell. However, due to the experimental  
378 conditions, where water does not cover the gel sample, but it is in contact with it only on the  
379 lateral side, this effect, if any, is negligible. It is well known, indeed, that the SR depends on  
380 the conditions and the effective free surface in contact with water.<sup>43</sup> The SR of the interface,  
381 estimated by measuring initial and final length of the gel is around 7% in 2 h. It was not  
382 possible to carry out a continuous time lapse for 24 h as the gel interface exceeded the field of  
383 view. However, it was possible to estimate a 24 h SR of the interface of approximately 20%.  
384 Obviously, this value of SR has not to be compared with SR reported above in Figure 1  
385 because in this case the SR is related only to one face of the sample, which is in direct contact  
386 with the solvent.

387



388

389 **Figure 7.** Schematic representation of the setup for permeation experiments of polystyrene  
 390 particles. (a) Swelling of the gel interface during 2h time lapse. Solid and dotted red lines  
 391 represent respectively, the initial interface and the swelling front of the gelatin gel. Diffusion  
 392 of 0.1  $\mu\text{m}$  (b) and 1  $\mu\text{m}$  (c) polystyrene particles in the gel after 24 h.

393

394 Regarding particle permeation, even if not fully appreciable from the images, the time lapse  
 395 shows that during the first two hours, particles do not start immediately to penetrate the gel  
 396 but it seems that due to the swelling, corresponding to a net displacement of the interface, the  
 397 latter is able to push particles in the swelling direction retarding their entrance. After 24 h,  
 398 however, it is possible to reconstruct the whole path of the particles inside the gel. Parts of  
 399 this path, reported in Figure 7b-c show that both particles penetrate the gel. Whilst 0.1  $\mu\text{m}$   
 400 particles diffuse through the entire sample reaching the second interface at a distance of about  
 401 6 mm, 1  $\mu\text{m}$  particles stop their run shortly after passing the interface. The distribution of  
 402 both particles in the gel is not uniform and the mean density is also significantly different,  
 403 with values of 0.04 and 0.01 for 0.1  $\mu\text{m}$  and 1  $\mu\text{m}$  particles, respectively, suggesting that 1  
 404  $\mu\text{m}$  particles diffuse but they are more affected by the network hindrance. The limited particle  
 405 penetration can be explained by considering that the distribution of pore dimension can be



406 highly heterogeneous. Considering also the further increase in mesh size due to swelling, it is  
 407 likely that both particles, even if with dimensions much larger than the average gelatin pores,  
 408 can find sufficiently large pores to pass through. Moreover, at least during swelling, it is  
 409 possible that the convective transport of the particles in water creates a stress concentration  
 410 around them, which can lead to further changes in network microstructure. These results,  
 411 together with the NMR experiments reported in the following section, suggest a new method  
 412 to improve drug-loading of gelatin gels used for drug delivery. In fact, one of the main  
 413 problems faced during drug-carriers encapsulation in gelatin gels is the formation of  
 414 aggregates, which strongly influence drug stability and release. The images of Figure 7, on  
 415 the contrary, show that particles, although distributed in a non-uniform manner, do not tend  
 416 to aggregate in clusters.

417

### 418 **Effect of polystyrene particles on the gelatin structure**

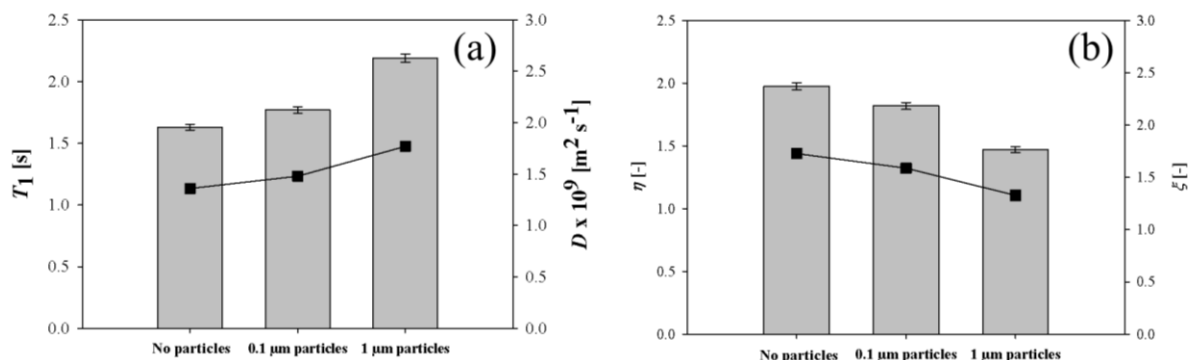
419 In order to understand the effect of particle penetration on the pore structure of the gel,  $T_1$  and  
 420 PFG NMR diffusion experiments were carried out on gelatin 30% samples in contact with  
 421 aqueous suspensions of polystyrene particles of 0.1 and 1  $\mu\text{m}$ . The results for  $T_1$  relaxation  
 422 times and self-diffusion coefficients,  $D$ , of water and the corresponding  $\eta$  and  $\xi$  parameters  
 423 for these samples are reported in Figure 8.

424

425

426

427



428

429 **Figure 8.** (a) Effect of solid particles on  $T_1$  relaxation time (columns) and self-diffusion  
430 coefficient  $D$  (squares) of water in gelatin 30% sample. (b) Effect of solid particles on  $\eta$   
431 (columns) and  $\xi$  (squares) parameters of water in gelatin 30%. For water behaving as free  
432 bulk water  $\eta$  and  $\xi$  are equal to one.

433

434 Figure 8a shows that the penetration of solid particles inside the gel is modifying the  $T_1$   
435 relaxation time and self-diffusion coefficient of water. In particular, larger particles  
436 contribute to an increase of both properties with a consequent decrease of  $\eta$  and  $\xi$  (Figure  
437 8b), which become closer to the value of one for free bulk water. It is possible that the  
438 penetration of solid particles inside the gel occurs through larger pores, which result in the  
439 observed increase for  $T_1$ , and at same time improves the pore network connectivity, hence  
440 enhancing diffusion within the pore network. It is reasonable that larger particles tend to  
441 cause more significant changes in pore structure and indeed, this is in line with the results  
442 reported in Figure 8.

443

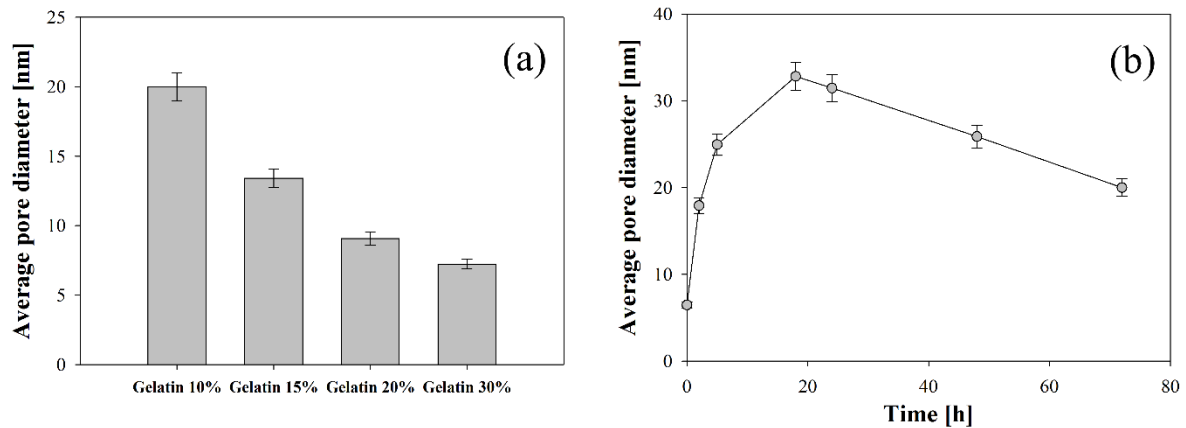
#### 444 **Estimation of average pore size**

445 Using the expression in Equation (4) and assuming the pores to be of cylindrical geometry,  
446 the observed  $T_1$  relaxation rate can be written as:

$$447 \quad \frac{1}{T_1} = \frac{1}{T_{1,\text{bulk}}} + \frac{4}{d} \rho_1 \quad (7)$$

448 where  $d$  is the average pore diameter. Therefore, if the surface relaxivity  $\rho_1$  is known, it  
449 becomes possible to calculate the average pore size of the porous gel from the observed  $1/T_1$   
450 relaxation rate values. The surface relaxivity can be estimated from Equation (7) using the  
451 value of observed  $T_1$  relaxation rate measured for the 10% gelatin sample and using the  
452 average pore diameter of 20 nm reported in the literature for this sample,<sup>38</sup> which gives  $\rho_1 \approx$   
453  $5.5 \times 10^{-4} \mu\text{m s}^{-1}$ . This value of surface relaxivity is significantly smaller than those reported  
454 in the literature for solid porous materials such as sandstones and other porous oxides<sup>44,45</sup> and  
455 this is largely expected given the absence of strong relaxation sinks such as paramagnetic  
456 ions and strong adsorption sites, which are typical of porous materials such as concrete, rocks  
457 and catalysts.<sup>45-47</sup> Once the surface relaxivity of the gelatin is estimated, it becomes possible  
458 to estimate the average pore size for the different samples using Equation (7). The values are  
459 reported in Figure 9 as a function of polymer concentration (Figure 9a) and for the gelatin

460 30% sample as a function of the swelling time (Figure 9b). The range for the calculated  
461 average pore diameter is in good agreement with the average pore size reported for these  
462 systems, which ranges from tens of nm down to a few nm.<sup>48-52</sup>



463

464 **Figure 9.** Average pore diameter calculated using Equation (7) for: (a) samples at different  
465 polymer concentration; (b) gelatin 30% sample as a function of the swelling time.

466

467 From Figure 9a it is possible to observe that as the polymer concentration is increased, the  
468 average pore size decreases to approximately 7 nm for the gelatin 30% samples. Figure 9b  
469 shows that the average pore diameter of the gelatin 30% sample increases more sharply in the  
470 first 5 hours of swelling, it then reaches a maximum at approximately 24 h, with an average  
471 pore size of approximately 32 nm, and then decreases reaching a value of approximately 20  
472 nm at 72 h. This behaviour is very similar to that observed for the swelling ratio, SR, and it  
473 suggests that SR and average pore diameter are closely related. Indeed, it is interesting to  
474 note that this behaviour is consistent with the trend observed for the swelling ratio, Figure 1,  
475 which also reaches a plateau but then undergoes a slight decrease at longer times. The  
476 similarity between these independent findings support the idea that the gelatin structure after  
477 an initial expansion may undergo some sort of relaxation of the pore structure, which results  
478 in a shrinkage with a consequent decrease of pore size.

479

## 480 CONCLUSIONS

481 In this work, NMR and CLSM are presented as insightful tools to investigate gelatin gel  
482 structures. The influence of the initial polymer concentration and swelling times are assessed.  
483 Firstly, the swelling ratio, SR, has been measured for four different gelatin samples in the

484 concentration range 10% - 30% (wt/wt) of gelatin. Results have shown that water uptake and  
485 corresponding SR is higher in the case of lower concentrations of gelatin. Moreover, it was  
486 interesting to note a slight weakness of the gelatin structure after equilibrium was reached,  
487 probably due to a starting relaxation of the network. NMR experiments have confirmed  
488 significant changes of relaxation and diffusion properties of water molecules as the polymer  
489 concentration increases. In particular, from the decrease in the  $T_1$  relaxation time of the fluid  
490 confined within the gelatin structure, due to an increase in polymer concentration, it is  
491 possible to observe an increase in surface-to-volume ratio of the pore structure, which is  
492 attributed to a reduction of the average pore dimension. Moreover, from NMR self-diffusion  
493 coefficients,  $D$ , it is possible to infer that the increase in polymer concentration causes also an  
494 increase of the tortuosity of the pore network. The effect of swelling time was also assessed.  
495 The initial rapid increase of both,  $T_1$  and  $D$  of water as a function of the swelling time  
496 suggests that water mobility is approaching that of the free bulk water, which is due to an  
497 increase in pore size and an improved pore network connectivity, i.e., decrease in tortuosity,  
498 and consequent enhancement of water mass transport by diffusion. However, at longer times  
499 both  $T_1$  and  $D$  values experience a slight but appreciable decrease which, in conjunction with  
500 the results on SR measurements, suggests that the gelatin structure is experiencing a slight  
501 shrinkage after a rapid initial expansion.

502 Further alterations of the gelatin structure have been demonstrated by analysing samples after  
503 penetration of polystyrene particles of 0.1 and 1  $\mu\text{m}$  diameter. Results have shown that both  
504 particles penetrate the gel structure, with the larger particles, in turn, affecting more the  
505 gelatin pore network and improving pore network connectivity. The limited number of pores  
506 larger than 1  $\mu\text{m}$  explains the lower mean concentration of 1  $\mu\text{m}$  particles compared to 0.1  
507  $\mu\text{m}$  particles. These results have been also supported by CLSM visualization, showing that 1  
508  $\mu\text{m}$  particles are able to slowly intercalate in the network, although they stop their permeation  
509 at a short distance from the interface. Finally, the average pore size, using  $T_1$  relaxation  
510 measurements, has been estimated in the range 7-21 nm for gelatin concentrations in the  
511 range 10%- 30%. The change in pore size of the 30% gelatin sample with swelling time was  
512 also estimated.

513 In conclusion, a combination of NMR and CLSM can reveal new insights into molecular  
514 dynamics and microstructure of gelatin and how this is affected by various parameters,  
515 including polymer composition, swelling ratio as well as the penetration of solid particles.  
516 Such knowledge is of importance for applications in many fields such as using gelatin as a  
517 drug-loading gel.

518

519

## 520 Acknowledgements

521 Carmine D'Agostino would like to acknowledge Wolfson College, Cambridge, for  
522 supporting his work and activities. Roberta Liuzzi would like to acknowledge Prof. Pietro  
523 Cicutta for the opportunity to stay at University of Cambridge and collaborate for this work.

524

## 525 References

- 526 1. M. Gómez-Guillén, J. Turnay, M. Fernández-Díaz, N. Ulmo, M. Lizarbe and P.  
527 Montero, *Food Hydrocolloids*, 2002, **16**, 25-34.
- 528 2. L. Ghasemi-Mobarakeh, M. P. Prabhakaran, M. Morshed, M.-H. Nasr-Esfahani and S.  
529 Ramakrishna, *Biomaterials*, 2008, **29**, 4532-4539.
- 530 3. S. Caserta, L. Sabetta, M. Simeone and S. Guido, *Chemical engineering science*, 2005,  
531 **60**, 1019-1027.
- 532 4. S. M. Tosh, A. G. Marangoni, F. R. Hallett and I. J. Britt, *Food Hydrocolloids*, 2003, **17**,  
533 503-513.
- 534 5. A. Duconseille, T. Astruc, N. Quintana, F. Meersman and V. Sante-Lhoutellier, *Food*  
535 *Hydrocolloids*, 2015, **43**, 360-376.
- 536 6. A. Karim and R. Bhat, *Trends in food science & technology*, 2008, **19**, 644-656.
- 537 7. A. Karim and R. Bhat, *Food hydrocolloids*, 2009, **23**, 563-576.
- 538 8. K. B. Djagny, Z. Wang and S. Xu, *Critical reviews in food science and nutrition*, 2001,  
539 **41**, 481-492.
- 540 9. S. Van Vlierberghe, P. Dubruel and E. Schacht, *Biomacromolecules*, 2011, **12**, 1387-  
541 1408.
- 542 10. B. V. Slaughter, S. S. Khurshid, O. Z. Fisher, A. Khademhosseini and N. A. Peppas,  
543 *Advanced materials*, 2009, **21**, 3307-3329.
- 544 11. E. Chong, T. Phan, I. Lim, Y. Zhang, B. Bay, S. Ramakrishna and C. Lim, *Acta*  
545 *biomaterialia*, 2007, **3**, 321-330.
- 546 12. T. Guo, J. Zhao, J. Chang, Z. Ding, H. Hong, J. Chen and J. Zhang, *Biomaterials*, 2006,  
547 **27**, 1095-1103.
- 548 13. S.-M. Lien, L.-Y. Ko and T.-J. Huang, *Acta Biomaterialia*, 2009, **5**, 670-679.
- 549 14. S. E. Kudaibergenov and V. B. Sigitov, *Langmuir*, 1999, **15**, 4230-4235.
- 550 15. C. H. Lee and Y. C. Bae, *Macromolecules*, 2015, **48**, 4063-4072.
- 551 16. C. Qiao and X. Cao, *Journal of Macromolecular Science, Part B*, 2014, **53**, 1609-1620.
- 552 17. M. Azami, M. Rabiee and F. Moztafzadeh, *Polymer Composites*, 2010, **31**, 2112-2120.
- 553 18. S.-M. Lien, W.-T. Li and T.-J. Huang, *Materials Science and Engineering: C*, 2008, **28**,  
554 36-43.
- 555 19. Q. Xing, K. Yates, C. Vogt, Z. Qian, M. C. Frost and F. Zhao, *Scientific reports*, 2014, **4**.
- 556 20. X. Lou and T. V. Chirila, *Journal of biomaterials applications*, 1999, **14**, 184-191.
- 557 21. R. H. Pritchard and E. M. Terentjev, *Polymer*, 2013, **54**, 6954-6960.
- 558 22. A. S. Hoffman, *Advanced drug delivery reviews*, 2012, **64**, 18-23.

- 559 23. H. Schott, *Journal of Macromolecular Science, Part B: Physics*, 1992, **31**, 1-9.
- 560 24. M. Gómez-Guillén, B. Giménez, M. a. López-Caballero and M. Montero, *Food*  
561 *Hydrocolloids*, 2011, **25**, 1813-1827.
- 562 25. X. Liu and P. X. Ma, *Biomaterials*, 2009, **30**, 4094-4103.
- 563 26. H.-W. Kang, Y. Tabata and Y. Ikada, *Biomaterials*, 1999, **20**, 1339-1344.
- 564 27. L. C. Dong, A. S. Hoffman and Q. Yan, *Journal of Biomaterials Science, Polymer*  
565 *Edition*, 1994, **5**, 473-484.
- 566 28. T. Brand, S. Richter and S. Berger, *The Journal of Physical Chemistry B*, 2006, **110**,  
567 15853-15857.
- 568 29. R. Dash, M. Foston and A. J. Ragauskas, *Carbohydrate polymers*, 2013, **91**, 638-645.
- 569 30. J. Maquet, H. Theveneau, M. Djabourov, J. Leblond and P. Papon, *Polymer*, 1986, **27**,  
570 1103-1110.
- 571 31. P. Belton, *International journal of biological macromolecules*, 1997, **21**, 81-88.
- 572 32. E. Fukushima, Roeder, S.W., *Experimental pulse NMR*, Addison-Wesley, Reading,  
573 US, 1981.
- 574 33. R. M. Cotts, M. J. R. Hoch, T. Sun and J. T. Markert, *Journal of Magnetic Resonance*,  
575 1989, **83**, 252-266.
- 576 34. J. E. Tanner, *Journal of Chemical Physics*, 1970, **52**, 2523-2526.
- 577 35. D. Biswal, B. Anupriya, K. Uvanesh, A. Anis, I. Banerjee and K. Pal, *Journal of the*  
578 *mechanical behavior of biomedical materials*, 2016, **53**, 174-186.
- 579 36. C. D'Agostino, J. Mitchell, L. F. Gladden and M. D. Mantle, *The Journal of Physical*  
580 *Chemistry C*, 2012, **116**, 8975-8982.
- 581 37. P. J. Barrie, *Annual Reports on NMR Spectroscopy*, 2000, **41**, 265-316.
- 582 38. S. Ma, M. Natoli, X. Liu, M. P. Neubauer, F. M. Watt, A. Fery and W. T. Huck, *Journal*  
583 *of Materials Chemistry B*, 2013, **1**, 5128-5136.
- 584 39. M. Dvoyashkin, R. Valiullin and J. Kärgler, *Physical Review* 2007, **75**, 041202.
- 585 40. M. D. Mantle, D. I. Enache, E. Nowicka, S. P. Davies, J. K. Edwards, C. D'Agostino, D. P.  
586 Mascarenhas, L. Durham, M. Sankar, D. W. Knight, L. F. Gladden, S. H. Taylor and G. J.  
587 Hutchings, *J. Phys. Chem. C*, 2011, **115**, 1073-1079.
- 588 41. F. Ganji, S. Vasheghani-Farahani and E. Vasheghani-Farahani, *Iran Polym J*, 2010, **19**,  
589 375-398.
- 590 42. D. Danino, R. Gupta, J. Satyavolu and Y. Talmon, *Journal of colloid and interface*  
591 *science*, 2002, **249**, 180-186.
- 592 43. C. Wu and C.-Y. Yan, *Macromolecules*, 1994, **27**, 4516-4520.
- 593 44. W. F. J. Slijkerman and J. P. Hofman, *Magnetic Resonance Imaging*, 1998, **16**, 541-  
594 544.
- 595 45. I. Foley, S. A. Farooqui and R. L. Kleinberg, *J. Magn. Reson. Ser. A*, 1996, **123**, 95-104.
- 596 46. C. D'Agostino, M. R. Feaviour, G. L. Brett, J. Mitchell, A. P. E. York, G. J. Hutchings, M.  
597 D. Mantle and L. F. Gladden, *Catalysis Science & Technology*, 2016, **6**, 7896-7901.
- 598 47. C. D'Agostino, J. Mitchell, M. D. Mantle and L. F. Gladden, *Chemistry - A European*  
599 *Journal*, 2014, **20**, 13009-13015.
- 600 48. S. M. Russell and G. Carta, *Industrial & engineering chemistry research*, 2005, **44**,  
601 8213-8217.
- 602 49. M. Helminger, B. Wu, T. Kollmann, D. Benke, D. Schwahn, V. Pipich, D. Faivre, D.  
603 Zahn and H. Cölfen, *Advanced functional materials*, 2014, **24**, 3187-3196.
- 604 50. M. Djabourov, N. Bonnet, H. Kaplan, N. Favard, P. Favard, J. Lechaire and M.  
605 Maillard, *Journal de Physique II*, 1993, **3**, 611-624.

- 606 51. Z. Yang, Y. Hemar, L. Hilliou, E. P. Gilbert, D. J. McGillivray, M. A. Williams and S.  
607 Chaieb, *Biomacromolecules*, 2015, **17**, 590-600.
- 608 52. M. A. da Silva, F. Bode, I. Grillo and C. c. A. Dreiss, *Biomacromolecules*, 2015, **16**,  
609 1401-1409.
- 610